membranes

MDPI

Article

Enhancing CO_2/N_2 and CO_2/CH_4 Separation Properties of PES/SAPO-34 Membranes Using Choline Chloride-Based Deep Eutectic Solvents as Additives

Jonathan S. Cardoso [1,*], Zhi Lin [2], Paulo Brito [3,4] and Licínio M. Gando-Ferreira [1,*]

[1] Chemical Engineering and Renewable Resources for Sustainability (CERES), Department of Chemical Engineering, Faculty of Sciences and Technology, University of Coimbra, Pólo II, Rua Sílvio Lima, 3030-790 Coimbra, Portugal
[2] Centre for Research in Ceramics and Composite Materials (CICECO), Department of Chemistry, University of Aveiro, 3810-193 Aveiro, Portugal; zlin@ua.pt
[3] Mountain Research Centre (CIMO), Polytechnic Institute of Bragança, Campus de Santa Apolónia, 5300-253 Bragança, Portugal; paulo@ipb.pt
[4] Associate Laboratory for Sustainability and Technology in Mountains Regions (SusTEC), Polytechnic Institute of Bragança, Campus de Santa Apolónia, 5300-253 Bragança, Portugal
* Correspondence: jonathancardoso@ipb.pt (J.S.C.); lferreira@eq.uc.pt (L.M.G.-F.)

Abstract: CO_2 separation is an important environmental method mainly used in reducing CO_2 emissions to mitigate anthropogenic climate change. The use of mixed-matrix membranes (MMMs) arrives as a possible answer, combining the high selectivity of inorganic membranes with high permeability of organic membranes. However, the combination of these materials is challenging due to their opposing nature, leading to poor interactions between polymeric matrix and inorganic fillers. Many additives have been tested to reduce interfacial voids, some of which showed potential in dealing with compatibility problems, but most of them lack further studies and optimization. Deep eutectic solvents (DESs) have emerged as IL substitutes since they are cheaper and environmentally friendly. Choline chloride-based deep eutectic solvents were studied as additives in polyethersulfone (PES)/SAPO-34 membranes to improve CO_2 permeability and CO_2/N_2 and CO_2/CH_4 selectivity. SAPO-34 crystals of 150 nm with a high surface area and microporosity were synthesized using dry-gel methodology. The PES/SAPO-34 membranes were optimized following previous work and used in a defined composition, using 5 or 10 w/w% of DES during membrane preparation. All MMMs were characterized by their ideal gas permeability using N_2 and CO_2 pure gasses. Selected membranes were also tested using CH_4 pure gas. The results presented that 5 w/w%, in polymer mass, of ChCl–glycerol presented the best result over the synthesized membranes. An increase of 200% in CO_2 permeability maintains the CO_2/N_2 selectivity for the non-modified PES/SAPO-34 membrane. A CO_2/CH_4 selectivity of 89.7 was obtained in PES/SAPO-34/ChCl-glycerol membranes containing 5 w/w% of this DES, which is an outstanding ideal separation performance for MMMs when compared to other results in the literature. FTIR analysis reiterates the presence of glycerol in the membranes prepared. Dynamic Mechanical Thermal Analysis (DMTA) shows that the addition of 5 w/w% of DES does not impact the membrane flexibility or polymer structure. However, in concentrations higher than 10 w/w%, the inclusion of DES could lead to high membrane rigidification without impacting the overall thermal resistance. SEM analysis of DES-enhanced membranes presented asymmetric final membranes and reaffirmed the results obtained in DMTA about rigidified structures and lower zeolite–polymer interaction with higher concentrations of DES.

Keywords: mixed-matrix membranes; PES; SAPO-34; deep eutectic solvents; interfacial voids

Citation: Cardoso, J.S.; Lin, Z.; Brito, P.; Gando-Ferreira, L.M. Enhancing CO_2/N_2 and CO_2/CH_4 Separation Properties of PES/SAPO-34 Membranes Using Choline Chloride-Based Deep Eutectic Solvents as Additives. *Membranes* **2024**, *14*, 230. https://doi.org/10.3390/membranes14110230

Academic Editor: Shing-Yi Suen

Received: 30 September 2024
Revised: 25 October 2024
Accepted: 31 October 2024
Published: 5 November 2024

1. Introduction

Emerging membrane technologies offer promising advantages for the separation of CO_2 from natural gas (CH_4) and air (N_2), including low energy consumption, ease of maintenance, straightforward operational control, low capital costs, and high energy efficiency. However, the broader adoption of polymeric membranes is limited by the inherent trade-off between selectivity and permeability, as depicted by Robeson's upper bound curve. In contrast, inorganic membranes exceed the upper bound in performance but are challenging to process. Consequently, the performance of mixed-matrix membranes (MMMs) depends on the selective properties of inorganic fillers, while the mechanical stability and ease of production provided by polymers enhance processing [1–4].

Numerous MMMs have been synthesized using various inorganic fillers, such as silicates, zeolites, carbon nanotubes, and metal–organic frameworks (MOFs), which are usually selected according to the separation intended to be performed [5–7]. In this regard, SAPO-34 was selected due to its selective properties and pore size (0.38 nm) near the kinetic diameter of CO_2 (0.33 nm), N_2 (0.364 nm), and CH_4 (0.38 nm), which are targets in this separation [8,9]. However, the presence of unselective voids caused by the incompatibility between organic matrix and inorganic fillers affects the separation performance of those MMMs. Attempts to enhance the compatibility led to the introduction of interactive functional groups on fillers [10–12].

Amine groups [13,14], silane groups [15,16], and ionic liquids [17,18] are the most used surface particle modifiers. Modifying the filler surface to enhance compatibility with the polymer is intended by adding functional groups or coatings to minimize chemical reactions or increase compatibility; several studies have attempted to use different surface modifiers to improve CO_2/CH_4 and CO_2/N_2 separation [19–24]. However, the emerging capabilities of deep eutectic solvents (DESs) arrive as a cheap and eco-friendly alternative to ionic liquids [25–29]. Ionic liquids (ILs) are salts that exist in a liquid state at relatively low temperatures composed of a combination of organic cations and organic or inorganic anions, presenting low volatility, high thermal stability, and conductivity [30,31]. Deep eutectic solvents (DESs) are a type of system that forms a liquid phase through a eutectic mixture of compounds. It is a combination of two or more components, typically a hydrogen bond donor (HBD) and a hydrogen bond acceptor (HBA), resulting in a substance with a melting point significantly lower than that of any of the individual component, strong intermolecular interaction between the components, biodegradability, non-toxicity, and thermal stability [32–35].

This work aimed to study the influence of choline chloride-based deep eutectic solvents in 5 *w*/*w*% and 10 *w*/*w*% concentrations, based on polymer mass, in a fixed optimized composition of a PES/SAPO-34 mixed-matrix membrane. The novelty of this study relies on how DESs can influence the final properties of MMM and if DESs are a real alternative to ionic liquids and other additives for mixed-matrix membranes. Ideal CO_2 and N_2 permeabilities were studied, and CH_4 in selected cases. Membranes incorporating less than 5 *w*/*w*% do not present expressive variation in CO_2/N_2 selectivity or CO_2 and N_2 permeability. Moreover, membranes containing 20 *w*/*w*% of DES were fabricated, but they did not meet the necessary criteria for further testing. The final membranes exhibited excessive porosity or degradation, attributed to the effects of DES inclusion. Changes in structure and chemical and thermal properties caused by the inclusion of DES during the membrane fabrication were analyzed, which is vital for explaining how DESs can interfere with the membrane characteristics and separation potential.

2. Results and Discussion

2.1. Characterization of PES/SAPO-34 Mixed-Matrix Membranes

PES/SAPO-34 membranes were prepared according to the methodology described in Section 3.2. DMTA and TGA were realized to compare thermal stability and flexibility based on the glass transition temperature for PES, PES/SAPO-34, and MMMs containing the 5 *w*/*w*% and 10 *w*/*w*% of DES, as depicted in Figures 1–3 and Figure A1, respectively.

DMTA, in Figure 1, presents the glass transition temperature (T_g) at a 1 Hz frequency of 234 °C and 219 °C for neat PES and PES/SAPO-34, respectively. Those temperatures express the flexibility degree of the membranes showing that the inclusion of SAPO-34 does not lead to a rigidified polymer/zeolite interface, since those rigidified interfaces would lead to a higher T_g than neat PES.

Figure 2 presents the glass transition temperature (Tg) at a 1 Hz frequency of 221 °C, 223 °C, and 198 °C for PES/SAPO-34/ChCl-urea, PES/SAPO-34/ChCl-glycerol, and PES/SAPO-34/ChCl-ethanolamine 5 *w*/*w*% concentrations. The T_g obtained for PES/SAPO-34/ChCl-urea and PES/SAPO-34/ChCl-glycerol are similar to that of the PES/SAPO-34 membrane. Moreover, the decrease in T_g for PES/SAPO-34/ChCl-ethanolamine shows that this concentration could lead to a more flexible membrane.

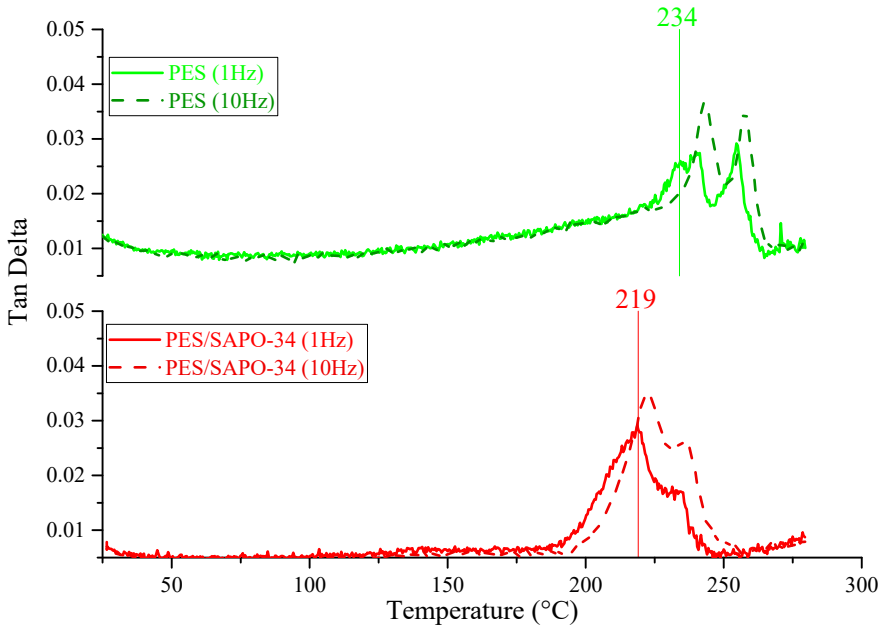

Figure 1. DMTA for PES and PES/SAPO-34 at 1 Hz and 10 Hz.

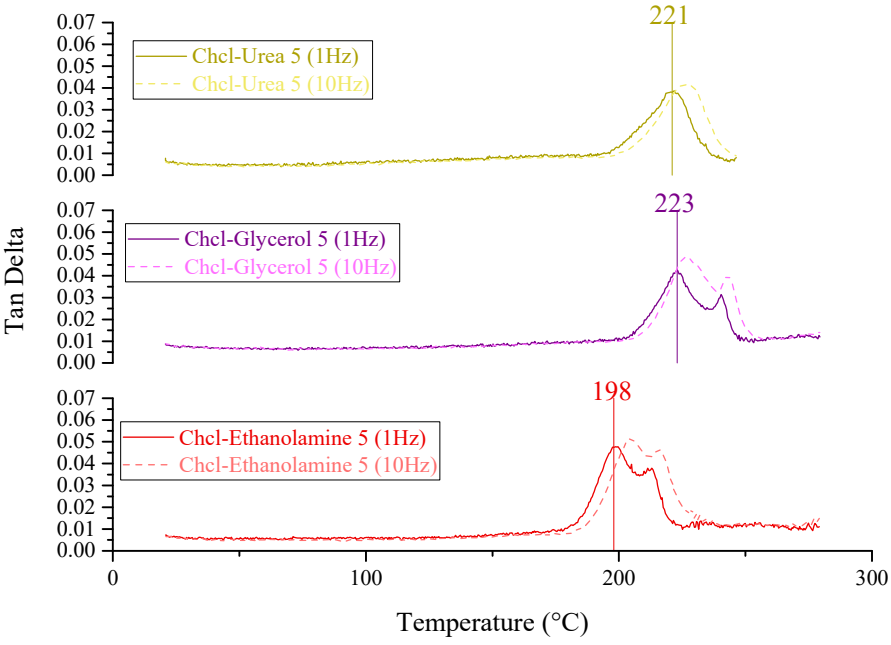

Figure 2. DMTA for PES/SAPO-34/DES using 5 *w*/*w*% at 1 Hz and 10 Hz.

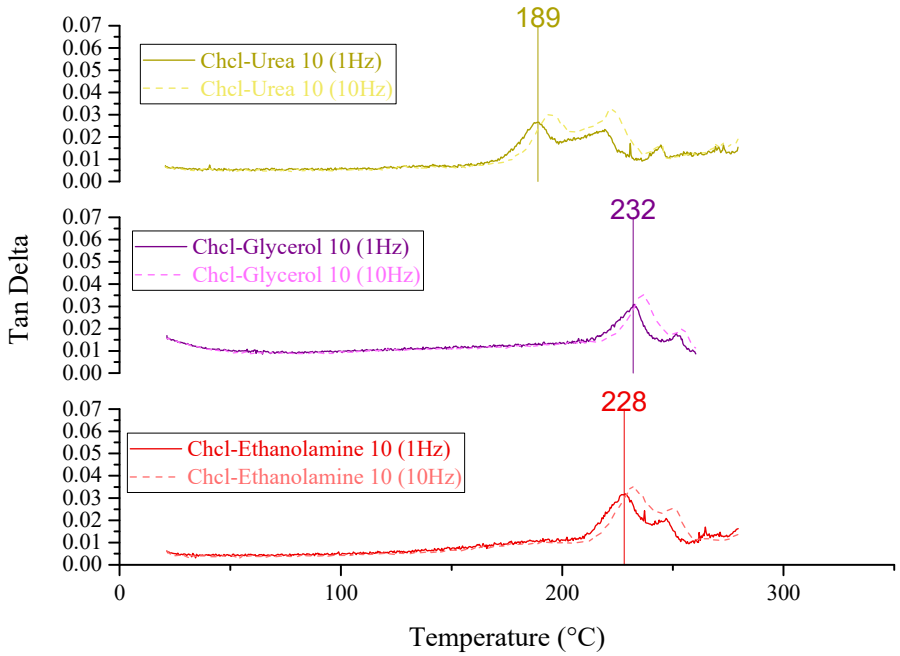

Figure 3. DMTA for PES/SAPO-34/DES using 10 w/w% at 1 Hz and 10 Hz.

Figure 3 presents the glass transition temperature (Tg) at a 1 Hz frequency of 189 °C, 232 °C, and 228 °C for PES/SAPO-34/ChCl-urea, PES/SAPO-34/ChCl-glycerol, and PES/SAPO-34/ChCl-ethanolamine 10 w/w% concentrations. The decrease in T_g with an increased concentration of ChCl–urea obtained for PES/SAPO-34/ChCl-urea is related to higher flexibility and more polymer chain mobility. The increased concentration of ChCl–glycerol and ChCl–ethanolamine in MMMs promoted a rigidified membrane structure that could lead to less particle–polymer interaction.

Figure A1 presents the TGA for the membranes prepared in this work to compare the thermal stability of neat PES and PES/SAPO-34 mixed-matrix membranes with the modified membranes containing 5 and 10 w/w% of different DESs. The degradation temperature for PES/SAPO-34 is 581 °C. It seems that 5 w/w% and 10 w/w% of DES were not enough to cause an impact on the thermal stability of the membranes prepared. The DES degraded around 250 °C as presented in Figures 2 and 3, which can also be observed in Figure A1 in the slight decrease in the same temperature scale.

Figure A2 presents the XRD for the membranes prepared with 5 w/w% of DESs compared to a neat PES membrane and a PES/SAPO-34 membrane without additives. CHA is the standard for characterizing SAPO-34 using XRD, endorsed by the International Zeolite Association (IZA). In CHA and SAPO-34, an identical tetrahedral structure is observed, with each tetrahedron coordinated by four oxygen atoms. These oxygen atoms serve as bridges between neighbouring tetrahedral atoms, resulting in a zeolite structure with uniform planes of dispersion. In Figure A2, the XRD obtained shows the neat PES pattern in all membranes and a CHA pattern of SAPO-34 with characteristic peaks in corresponding diffraction angles as the CHA standard diffractogram. The patterns of PES/SAPO-34 membranes with and without DES treatment are very similar. They are a combination of polymer and SAPO-34. The DES treatment did not influence the patterns.

Moreover, Figures A3–A5 present the FTIR analysis for the membranes prepared and compared with the PES/SAPO-34 membrane and deep eutectic solvents related to those membranes. All membranes presented the three peaks observed at 1576–1577 cm^{-1}, 1482–1484 cm^{-1}, and 1405–1406 cm^{-1}, indicating the presence of benzene rings. The two peaks at 1320–1321 cm^{-1} and 1296–1297 cm^{-1} indicate the presence of ether function. The two peaks at 1144–1146 cm^{-1} and 1100–1101 cm^{-1} indicate the presence of the sulfone group. All spectra are according to FTIR spectra for PES in the literature. The band between

1080 and 1015 cm^{-1} is related to Si-O and Al-O vibration and implies the addition of SAPO-34. The difference in the spectra's shape between the PES/SAPO-34 and PES/SAPO-34/DES membranes in the range 1050–900 cm^{-1} denotes the existence of ChCl in the membrane since this alteration occurred in all membranes where ChCl was used and corresponds to the expected results since ChCl tends to degrade at 303 °C [36,37].

In Figure A3, no peaks characterizing urea could be found in the spectra for those membranes, suggesting the degradation of this compound after membrane drying [38].

In Figure A4, the peaks presented in 3291 cm^{-1}, 3027 cm^{-1}, 952 cm^{-1}, and 923 cm^{-1} could be related to glycerol combined with ChCl, which is more present in the PES/SAPO-34/glycerol 10 w/w% membrane, suggesting the presence of this compound after membrane drying since glycerol degrades at 290 °C [39].

In Figure A5, the peak presented in 3600–3000 cm^{-1} is related to an OH band, and this could be related to ethanolamine presence. Although, ethanolamine's degradation temperature is 167 °C, the OH bandwidth presented in the spectra is the product from that degradation [40].

SEM analysis results for the PES/SAPO-34 and PES/SAPO-34/DES membranes containing 5 w/w% and 10 w/w% of the additives are presented in Figures 4–10, respectively, depicting the membrane surface; cross-section of the general structure used to evaluate the crystal dispersion; and zoom-in of the particle–polymer interaction.

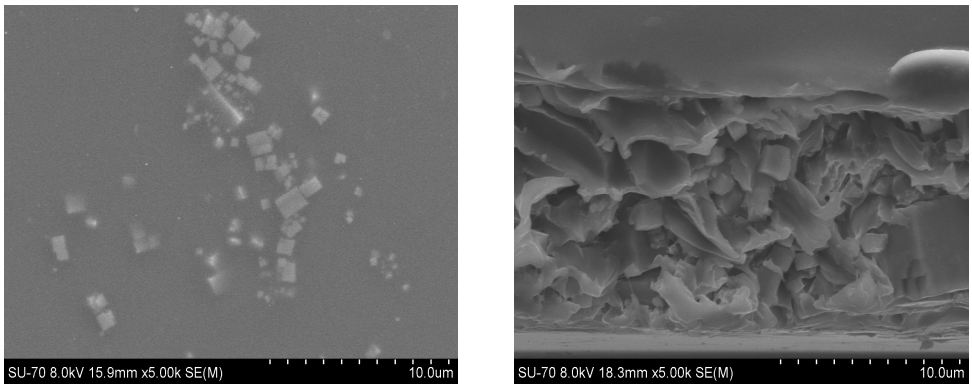

(**a**) (**b**)

Figure 4. (**a**) Surface and (**b**) cross-section of PES/SAPO-34 membrane.

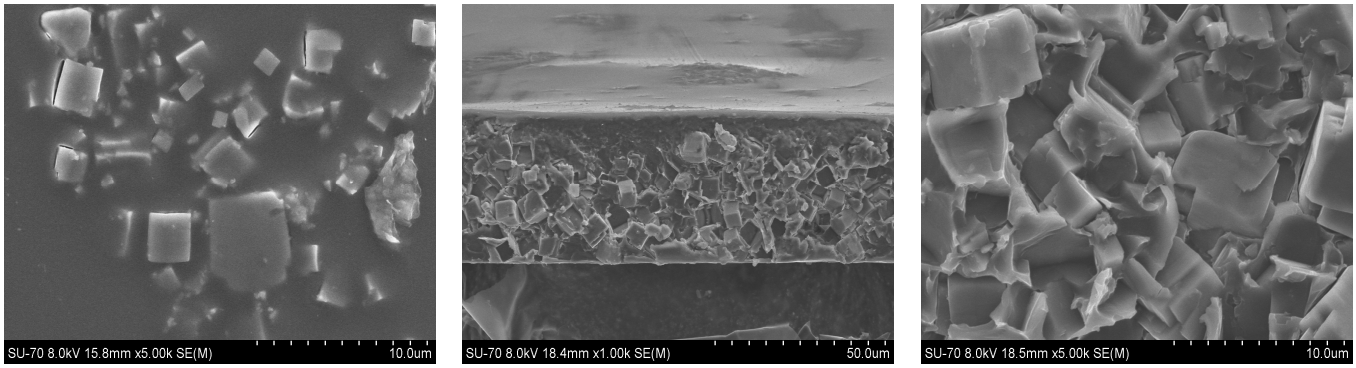

(**a**) (**b**) (**c**)

Figure 5. (**a**) Surface, (**b**) cross-section, and (**c**) zoom-in of particles in cross-section of PES/SAPO-34/ChCl-urea 5 w/w% membrane.

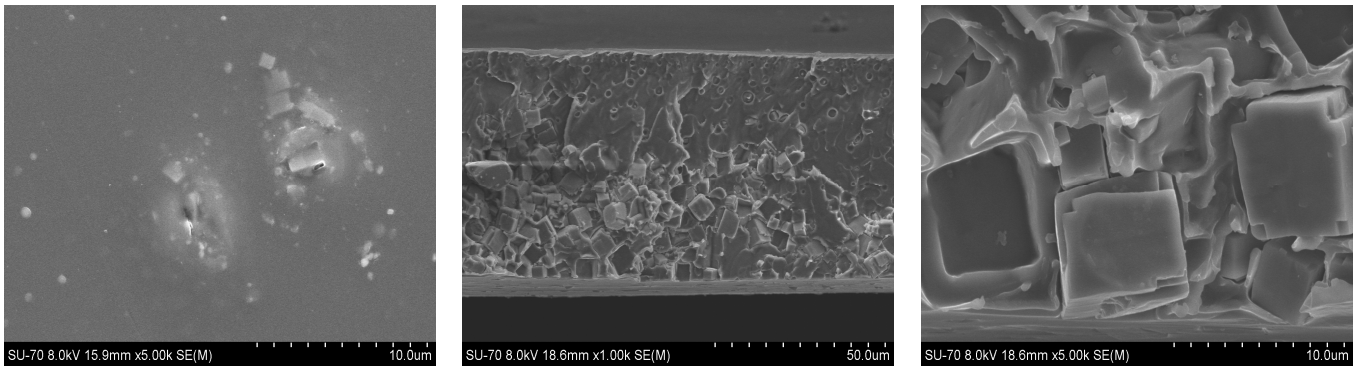

(**a**) (**b**) (**c**)

Figure 6. (**a**) Surface, (**b**) cross-section, and (**c**) zoom-in of particles in cross-section of PES/SAPO-34/ChCl-glycerol 5 *w*/*w*% membrane.

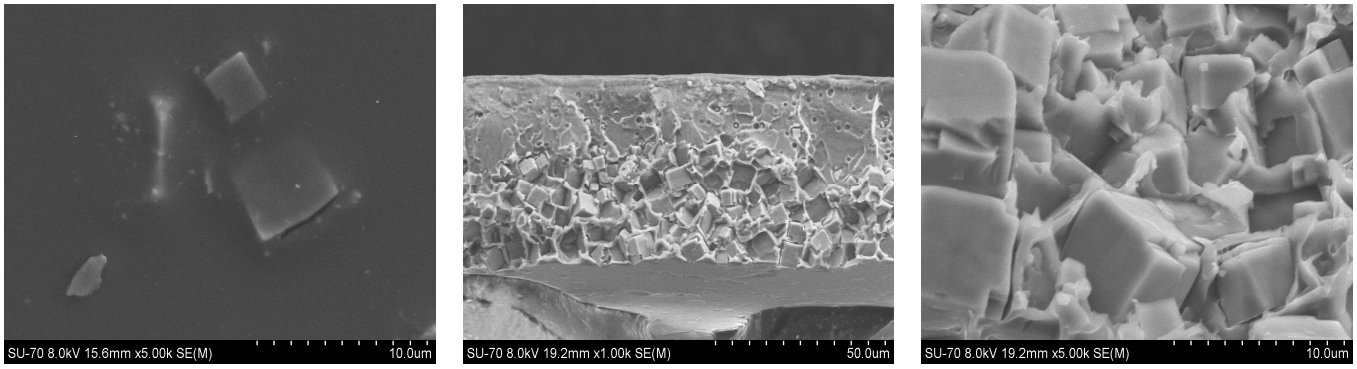

(**a**) (**b**) (**c**)

Figure 7. (**a**) Surface, (**b**) cross-section, and (**c**) zoom-in of particles in cross-section of PES/SAPO-34/ChCl-ethanolamine 5 *w*/*w*% membrane.

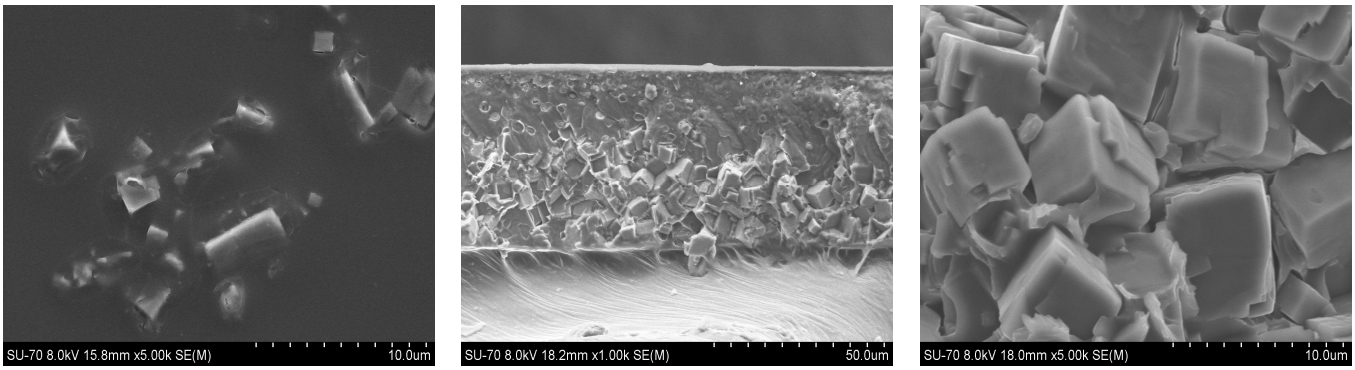

(**a**) (**b**) (**c**)

Figure 8. (**a**) Surface, (**b**) cross-section, and (**c**) zoom-in of particles in cross-section of PES/SAPO-34/ChCl-urea 10 *w*/*w*% membrane.

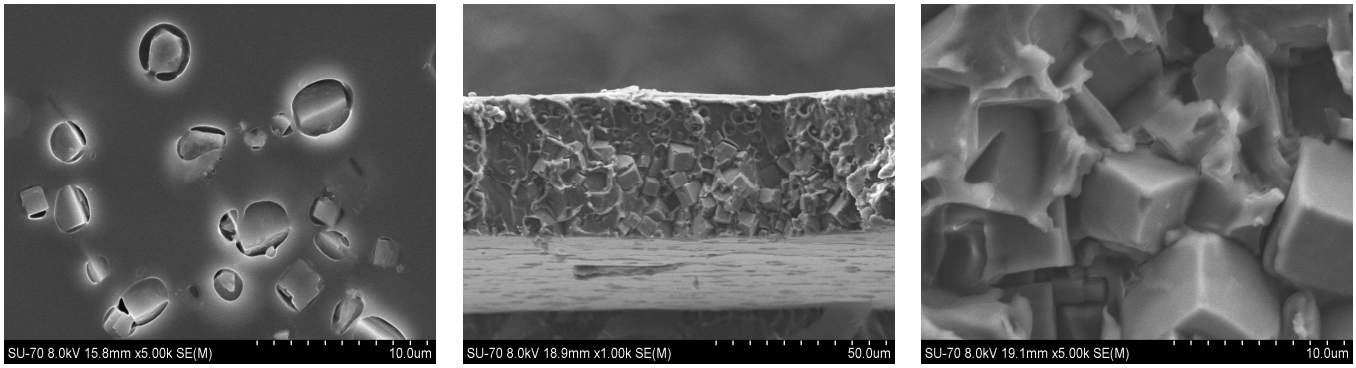

(**a**) (**b**) (**c**)

Figure 9. (**a**) Surface, (**b**) cross-section, and (**c**) zoom-in of particles in cross-section of PES/SAPO-34/ChCl-glycerol 10 *w*/*w*% membrane.

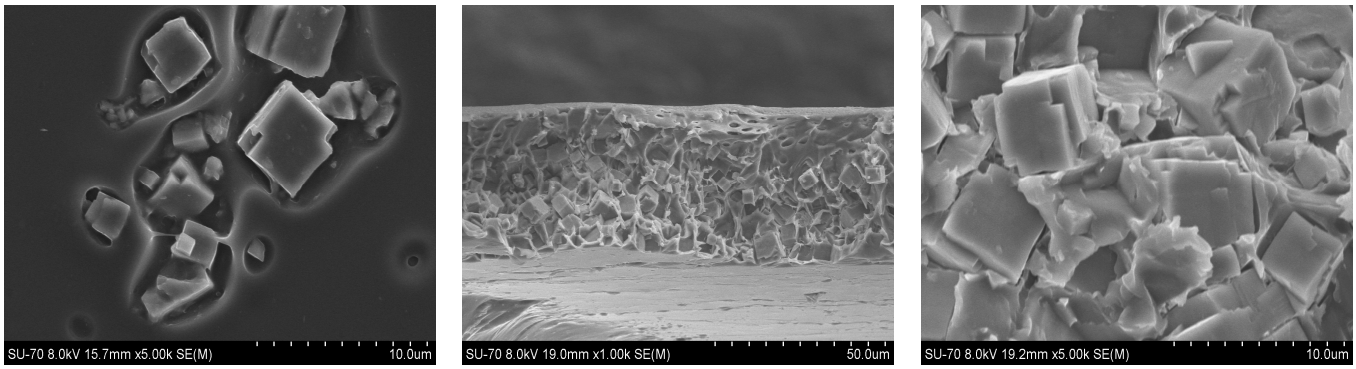

(**a**) (**b**) (**c**)

Figure 10. (**a**) Surface, (**b**) cross-section, and (**c**) zoom-in of particles in cross-section of PES/SAPO-34/ChCl-ethanolamine 10 *w*/*w*% membrane.

Figure 4a presents the PES/SAPO-34 membrane surface with crystals dispersed all over. Figure 4b presents the SEM analysis of the PES/SAPO-34 membrane cross-section, and the agglomeration of crystals with the polymeric matrix can be seen.

Figures 5–10 present the SEM analysis of the PES/SAPO-34 membrane containing 5 and 10 *w*/*w*% of ChCl–urea, ChCl–glycerol, and ChCl–ethanolamine additives. Figures 5a, 6a, 7a, 8a, 9a and 10a present a similar surface characterized by the presence of crystals.

In Figures 5b, 6b, 7b, 8b, 9b and 10b, the cross-section of membranes with additives presented a higher concentration of crystals in the bottom phase. The addition of DES reduced the polymer viscosity, enabling the zeolite crystals to more easily precipitate inside the polymer matrix. Although this precipitation caused a higher concentration of particles on one side, forming an asymmetric membrane, it is worth pointing out that the particles were all covered by the polymer. This interaction seems stronger with the 5 *w*/*w*% DES concentration. Furthermore, an increase in the DES concentrations from 5 to 10 *w*/*w*% led to a rigidified polymer structure, as shown in Figure 3, consequently occluding the particles and reducing the particle–polymer interaction, which is more evident in Figures 5c, 6c, 7c, 8c, 9c and 10c, which presents a zoom-in of the particles for each membrane. The interaction between the particles and polymer seems better in membranes containing 5 *w*/*w*% of DES in comparison to membranes with 10 *w*/*w*%.

2.2. Gas Permeation Tests

The films were submitted to a permeation test using CO_2 and N_2 pure gasses, and in selected membranes, CH_4 was used. CO_2 and N_2 permeabilities and the ideal CO_2/N_2

selectivity were obtained using Equations (1) and (2); the average values are presented in Table 1.

Table 1. Comparison of the CO_2/N_2 separation performance of PES, PES/SAPO-34, PES/SAPO-34/ChCl-urea, PES/SAPO-34/ChCl-glycerol, and PES/SAPO-34/ChCl-ethanolamine membranes.

Sample	*w*/*w*% DES	$\alpha CO_2/N_2$	PCO_2 (Barrer)	PN_2 (Barrer)
Neat PES	0	21.35 ± 3.62	1.04 ± 0.003	0.05 ± 0.009
PES/SAPO-34	0	29.96 ± 0.67	0.75 ± 0.11	0.025 ± 0.0004
PES/SAPO-34/ChCl-urea	5	10.92 ± 2.03	0.35 ± 0.07	0.032 ± 0.0001
	10	6.21 ± 0.73	0.86 ± 0.07	0.139 ± 0.01
PES/SAPO-34/ChCl-glycerol	5	29.63 ± 2.57	1.37 ± 0.12	0.046 ± 0.00002
	10	13.49 ± 0.33	1.01 ± 0.04	0.075 ± 0.01
PES/SAPO-34/ChCl-ethanolamina	5	11.22 ± 0.29	0.48 ± 0.09	0.043 ± 0.01
	10	8.43 ± 0.46	0.98 ± 0.08	0.115 ± 0.003

In Table 1, a comparison between the neat PES and PES/SAPO-34 membranes reveals a reduction in the CO_2 and N_2 permeabilities. This reduction can be attributed to adding molecular sieving materials, which introduce an extended diffusion pathway. This extended pathway arises if the molecular sieve mechanism is the limiting process, as it compels molecules to traverse a longer distance compared to neat polymer membranes. The elongated path through the polymer (via the solution–diffusion mechanism) and the material's pore structure (via the molecular sieve mechanism) results in prolonged permeation times, leading to lower permeability. However, despite this decrease in permeability, the properties of the molecular sieve material contribute to an increase in selectivity by more effectively retaining larger molecules [41,42].

The inclusion of choline chloride–urea and choline chloride–ethanolamine at a concentration of 5 *w*/*w*% resulted in a decrease in CO_2 permeability. Conversely, choline chloride–glycerol at the same concentration led to an increase in CO_2 permeability, as depicted in Figure 11a, while maintaining the CO_2/N_2 selectivity of the unmodified PES/SAPO-34 membrane, as shown in Figure 11b. Upon comparing the results obtained from gas permeation tests—Dynamic Mechanical Thermal Analysis (DMTA), Figure 2; FTIR, Figure A4; and scanning electron microscopy (SEM) analysis, Figures 5–7—it can be inferred that the addition of 5 *w*/*w*% of deep eutectic solvent (DES) enhanced the interaction between particles and polymer, thereby preserving the original characteristics of the PES/SAPO-34 membrane.

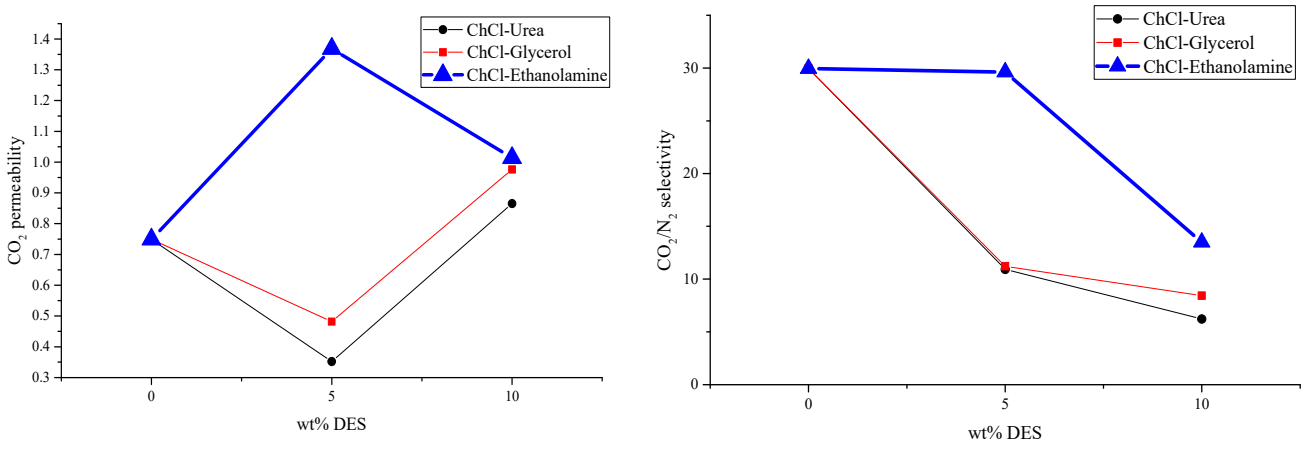

(**a**) (**b**)

Figure 11. Comparison of the impact on (**a**) CO_2 permeability and (**b**) CO_2/N_2 selectivity according to the amount of DES added.

Increasing the DES concentration to 10 *w*/*w*% increased CO_2 permeability for choline chloride–urea and choline chloride–ethanolamine. In contrast, a reduction in CO_2 permeability was observed when increasing the concentration of choline chloride–glycerol from 5 to 10 *w*/*w*%. In comparing the results obtained from gas permeation tests (DMTA in Figure 3, and SEM analysis in Figures 8–10), it can be deduced that the addition of 10 *w*/*w*% of DES promoted a rigidified polymer structure at the particle–polymer interface, as indicated by the increase in the glass transition temperature (Tg) in Figure 3 and the overall structural changes in Figures 8–10. This rigidified region may lead to diminished interaction between polymer and particles, ultimately resulting in increased CO_2 permeability for all membranes and a reduction in CO_2/N_2 selectivity, as illustrated in Table 1 and Figure 11b.

Among all PES/SAPO-34/DES membranes evaluated, the MMM containing 5 *w*/*w*% of ChCl–glycerol presented the best result, as shown in Figure 12, with double the CO_2 permeability with a CO_2/N_2 selectivity similar to that of the non-modified PES/SAPO-34 membrane. The MMMs containing ChCl–glycerol were tested for CO_2/CH_4 separation. The results obtained are presented in Table 2 and Figure 13, showing that a high CO_2 permeability was obtained with outstanding CO_2/CH_4 selectivity in PES/SAPO-34/ChCl-glycerol 5 *w*/*w*% when compared to other SAPO-34 MMMs in the literature.

The CO_2/CH_4 selectivity presented in Table 2 for PES/SAPO-34/ChCl-Glycerol 5 and 10 *w*/*w*% is on par with the expected results; CH_4 having a larger kinetic diameter than N_2 results in a higher separation performance of the pair CO_2/CH_4 compared to CO_2/N_2. PES/SAPO-34/ChCl-glycerol 5 *w*/*w*% showed outstanding CO_2/CH_4 selectivity with higher CO_2 permeability when compared with the PES/SAPO-34 membrane. Figure 13 compares the ideal performance with other results in the literature.

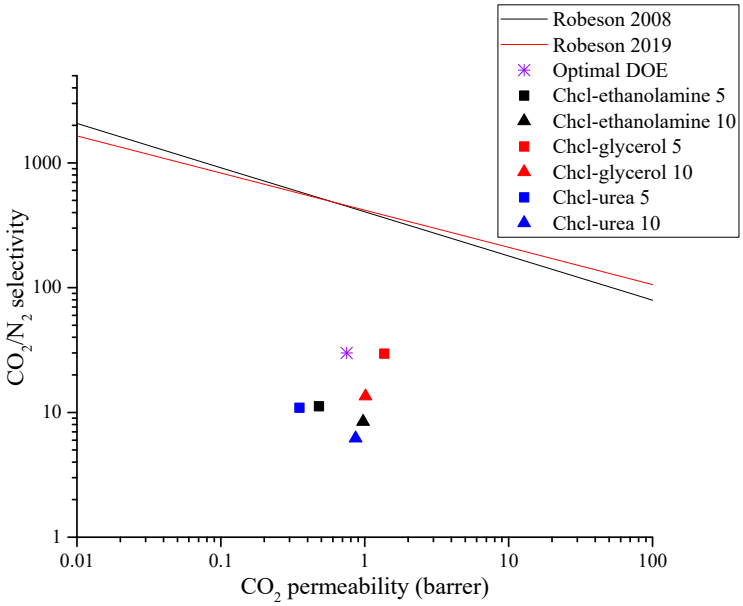

Figure 12. CO_2/N_2 Robeson upper bound [1,3] and a comparison of this work with SAPO-34 mixed-matrix membranes results.

Table 2. Comparison in CO_2/CH_4 separation performance of 5 and 10 *w*/*w*% PES/SAPO-34/ChCl-Glycerol membranes.

Sample	*w*/*w*% DES	$\alpha CO_2/CH_4$	PCO_2 (Barrer)	PCH_4 (Barrer)
PES/SAPO-34/ChCl-Glycerol	5	89.70 ± 5.24	1.37 ± 0.12	0.02 ± 0.00043
	10	35.77 ± 0.62	1.01 ± 0.04	0.028 ± 0.001

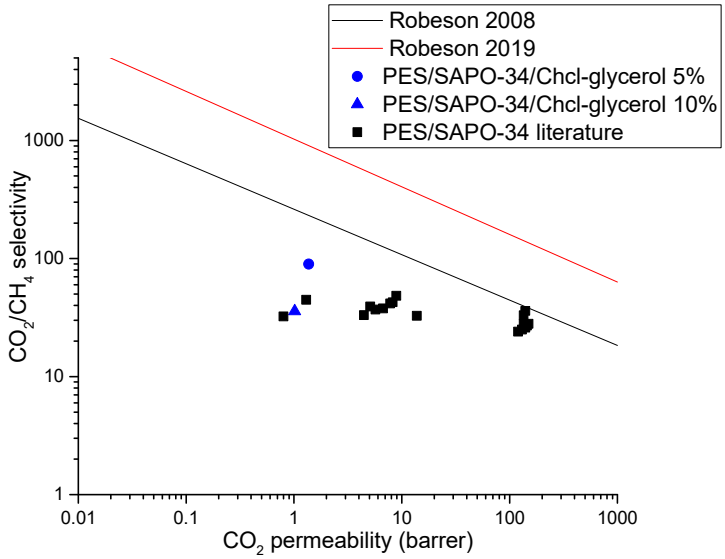

Figure 13. CO_2/CH_4 Robeson upper bound [1,3] and a comparison of this work with SAPO-34 mixed-matrix membranes results in the literature [42–45].

3. Materials and Methods

3.1. Materials

The polymer used in this study was polyethersulfone (PES) from Goodfellow: transparent, 3 mm granular size, and molecular weight of 58,000 g/mol. It was used as the media for the membrane. The inorganic filler SAPO-34 was prepared using Aluminum isopropoxide (≥99% purity), phosphoric acid (85%), colloidal silica HS-40, morpholine (≥99% purity), and Tetraethylammonium hydroxide (TEAOH) solution (35 wt% in water) purchased from Sigma–Aldrich (St. Louis and Burlington, MA, USA) following the procedure used in a previous work [46]. PES and SAPO-34 were dried overnight at 105 °C and 200 °C, respectively, prior to use. The solvent used for membrane preparation and casting was N-methyl-pyrroline (NMP) (≥99.8% purity) from Roth. Choline chloride (ChCl) (≥98% purity), urea (≥99.5% purity), glycerol, and ethanolamine (99% purity), from Sigma-Aldrich, were used to prepare the respective deep eutectic solvents (DESs) following the molar composition shown in Table 3.

Table 3. Deep eutectic solvent ratio.

Reagents	Molar Ratio	DES	T (K)	P (Bar)	xCO_2
ChCl Urea	1:2	1ChCl/2Urea	313–333	10.0–127.3	5.1–30.9
ChCl Glycerol	1:2	1ChCl/2Glycerol	303–343	1.9–63.5	0.6–39.9
ChCl Ethanolamine	1:6	1ChCl/6Ethanolamine	298	10.0	11.0

All DESs were selected due to their CO_2 adsorption properties and prepared by weighing the corresponding amount for each molar ratio and mixing at 70 °C until a homogeneous solution was formed, and then cooled down [27,29,32,47].

3.2. Synthesis of PES/SAPO-34 Mixed-Matrix Membranes

PES/SAPO-34 membranes were prepared according to the mass composition of 15 wt% of PES and 18.5 wt% of SAPO-34, based on polymer mass in NMP; this was an optimal composition for the CO_2/N_2 separation developed in our previous work [48]. The SAPO-34 zeolite was added and stirred with N-Methyl-2-pyrrolidone (NMP) for 1 h and in an ultrasonic bath for 4 h. Then, a small quantity of PES was added to the NMP/SAPO-34

solution and mixed for 1 h at room temperature. The remaining PES was added and mixed until complete solubilization, and the solution was stirred overnight. The solutions were degassed for 1 h in ultrasonic bath and cast with a knife of 400 µm of initial thickness, dried at 90 °C for 8 h and at 200 °C for 20 h under vacuum. Membranes containing the deep eutectic solvents followed the same procedure. The DESs were previously prepared separately and the necessary amount, 5 or 10 *w*/*w*% of each DES, was added during the NMP/SAPO-34 mixing. The final thickness of the dried membranes was 50–60 µm.

3.3. Gas Permeation Experiments

Gas permeation experiments were conducted using pure gasses to determine their ideal permeability and diffusivity coefficients, and the results were compared to each other in a permeability unit called Barrer (10^{-10}cm$^3_{STP} \cdot$ cm/cm$^2 \cdot$ s $\cdot$ cmHg). The membranes were cut into 18 mm discs mounted on a steel permeation cell and tested at a feed pressure of 10 bar at room temperature. The permeabilities were obtained according to Equation (1).

$$P_i = \frac{V_s l}{T_{AMB} \Delta p} \frac{T_{STP}}{p_{STP} A} \frac{dp}{dt} \quad (1)$$

The permeability of a certain gas (P_i) is related to the thickness of the film (l), the fixed volume of the permeate (Vs), which is measured as standard. The ambient temperature is T_{AMB}; the difference in pressure between the permeate and retentate, Δp; the permeation area, A; and the temperature and pressure in normal conditions, T_{STP} and P_{STP}. The ideal selectivity results (α_{ab}) are represented by the ratio between the permeability (P) of two pure gasses, a and b, respectively, measured separately under the same conditions in the same membrane to evaluate the separation performance, as presented in Equation (2).

$$\alpha_{ab} = \frac{P_a}{P_b} \quad (2)$$

3.4. Characterization of PES/SAPO-34 Mixed-Matrix Membranes

The samples were characterized by a Dynamic Mechanical and Thermal Analysis (DMTA) using Triton Technology equipment, Leicestershire, UK, model Tritec 2000, with a heating rate of 2 °C/min in 1 and 10 Hz frequencies for all samples to verify the glass transition temperature, as well as a Thermogravimetric Analysis (TGA) using a TA Instruments TGA Q500 with an N2 flow of 10 mL/min at 10 °C/min to obtain the degradation temperatures. Fourier-transform infrared spectroscopy (FTIR) was used to compare the presence or absence of chemical components and alterations. A total attenuated reflectance non-destructive technique (ATR) was used in the range of 4000–550 cm^{-1} in a Perkin Elmer spectrometer model Spectrum Two FT-IR with a DTGS detector and a KBr beam-splitter, a resolution of 4.0 cm^{-1}, 64 scans, and 50 N of constant applied force. Scanning electron microscopy (SEM) using a Hitachi SU-70 microscope was conducted to compare the membrane structure, morphology, and zeolite dispersibility, and a Contact Angle analysis was performed using Dataphysics equipment, a Contact Angle System OCA model, Filderstadt, Germany.

4. Conclusions

This work aimed to study the influence of choline chloride-based deep eutectic solvents containing urea, glycerol, or ethanolamine as additives into mixed-matrix membranes. Those DESs were added in situ during solution preparation in concentrations of 5 *w*/*w*% and 10 *w*/*w*%, based on polymer mass, in a fixed optimized composition of PES/SAPO-34 mixed-matrix membrane. FTIR analysis revealed the presence of glycerol in the membrane structures prepared. However, it also denoted the absence of urea and ethanolamine. DMTA showed that the addition of DES could lead to high membrane rigidification. While the addition of 5 *w*/*w*% of DES does not cause high disturbance in the polymer's overall structure and flexibility, which helps with improving the accommodation of the crystal with

a more flexible polymer, concentrations higher than 10 w/w% of DES disrupt the membrane stability, causing high rigidification processes and leading to less selective membranes. However, those additives did not prejudice the thermal stability of the membranes; as presented in the TGA results, they affect the membrane separation performance. DES concentrations of 20 w/w% or higher cause an increased porosity and a deformed membrane structure. Moreover, SEM analysis revealed an asymmetric membrane structure and reinforced the results in DMTA where DES-incorporated membranes led to rigidified structures and lower zeolite–polymer interaction with higher concentrations of DES. FTIR analysis clarified that DES with components with higher degradation temperature could resist the membrane drying procedure, resulting in more selective and permeable MMMs.

The gas permeation results showed that the PES/SAPO-34 membrane containing 5 w/w% of ChCl–glycerol presented increased CO_2 permeability due to CO_2 affinity and similar CO_2/N_2 selectivity when compared to a non-modified PES/SAPO-34 membrane. Further tests using pure CH_4 also revealed high CO_2/CH_4 selectivity when compared to other SAPO-34 membranes presented in the literature, which ultimately resulted in a membrane with an outstanding CO_2/CH_4 ideal separation performance.

Furthermore, deep eutectic solvents can act as additives to improve membrane performance as a more eco-friendly and less expensive alternative. However, further studies are necessary to compare the use of the same membrane composition and different additives to evaluate the performance of particle surface modification.

Author Contributions: Conceptualization, J.S.C., Z.L., P.B. and L.M.G.-F.; investigation, J.S.C.; resources, Z.L., P.B. and L.M.G.-F.; writing—original draft preparation, J.S.C.; writing—review and editing, J.S.C., Z.L., P.B. and L.M.G.-F.; visualization, J.S.C.; supervision, Z.L., P.B. and L.M.G.-F.; project administration, Z.L., P.B. and L.M.G.-F.; funding acquisition, J.S.C., Z.L., P.B. and L.M.G.-F. All authors have read and agreed to the published version of the manuscript.

Funding: The authors gratefully acknowledge the fundings from the Strategic Project of CERES (UIDB/00102/2020), CICECO-Aveiro Institute of Materials (UIDB/50 011/2020, UIDP/50 011/2020, and LA/P/0 0 06/2020), CIMO (UIDB/00690/2020 and UIDP/00690/2020), and SusTEC (LA/P/0007/2021), financed by the Fundação para a Ciência e Tecnologia (FCT) through national funds. J. S. Cardoso is also grateful for the financial support of the FCT through PhD grants (SFRH/BD/148170/2019 and COVID/BD/153647/2024).

Institutional Review Board Statement: Not applicable.

Informed Consent Statement: Not applicable.

Data Availability Statement: All data underlying the results are available as part of the article, and no additional source data are required.

Acknowledgments: The authors gratefully acknowledge the support from CERES, University of Coimbra, CICECO—Aveiro Institute of Materials; CIMO—Montain Research Centre; SusTEC—Associate Laboratory for Sustainability and Technology in Mountains Regions; and FCT—Fundação para a Ciência e Tecnologia.

Conflicts of Interest: The authors declare no conflicts of interest.

Appendix A

In this section, the results obtained by TGA (Figure A1), membrane XRD (Figure A2), and FTIR for all membranes prepared are represented in Figures A3–A5.

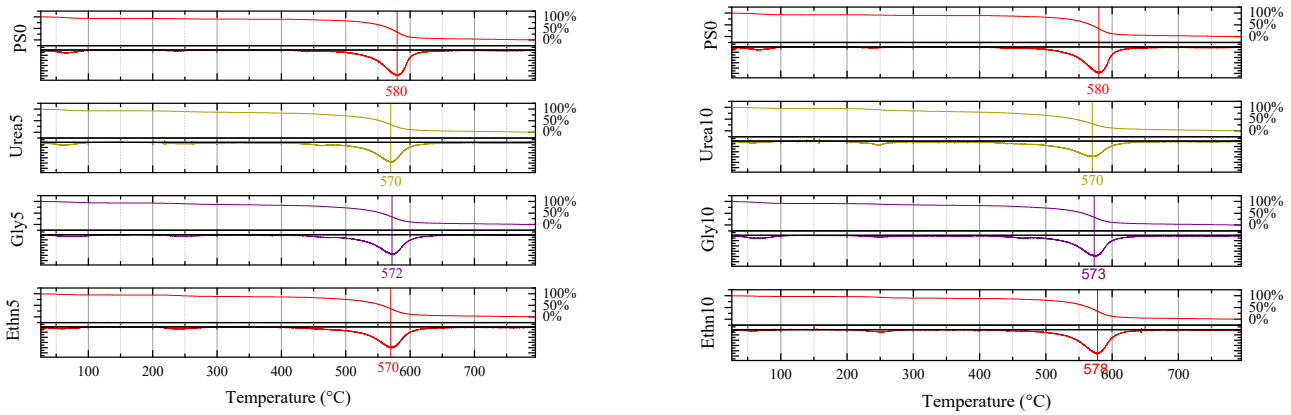

Figure A1. TGA for PES/SAPO-34 and PES/SAPO-34/DES membranes containing (**a**) 5 w/w% and (**b**) 10 w/w% of each DES.

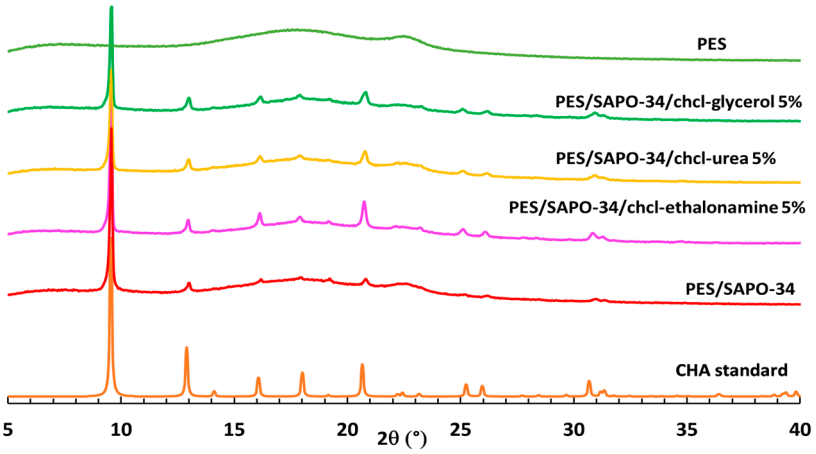

Figure A2. XRD for PES/SAPO-34 and PES/SAPO-34/DES membranes with 5 w/w% of DES.

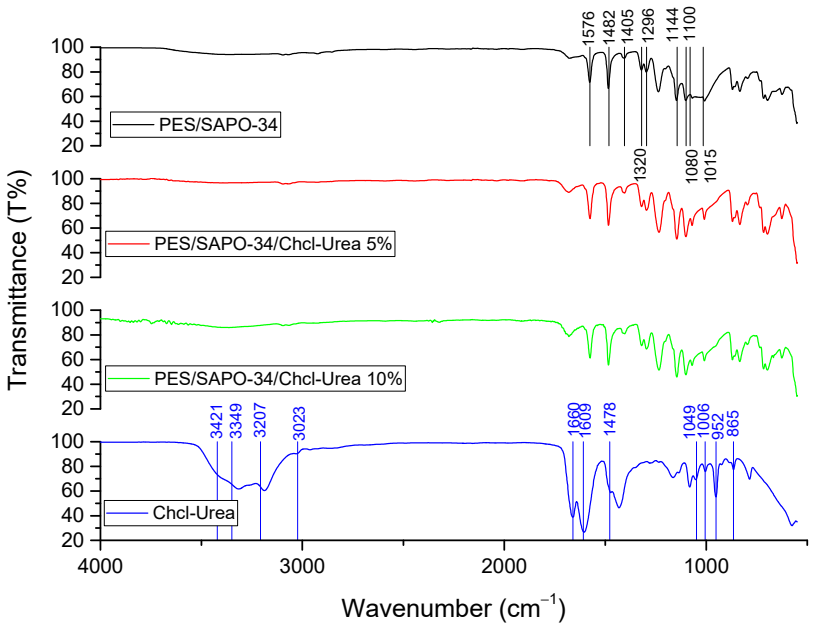

Figure A3. FTIR for PES/SAPO-34 and PES/SAPO-34/ChCl–urea membranes.

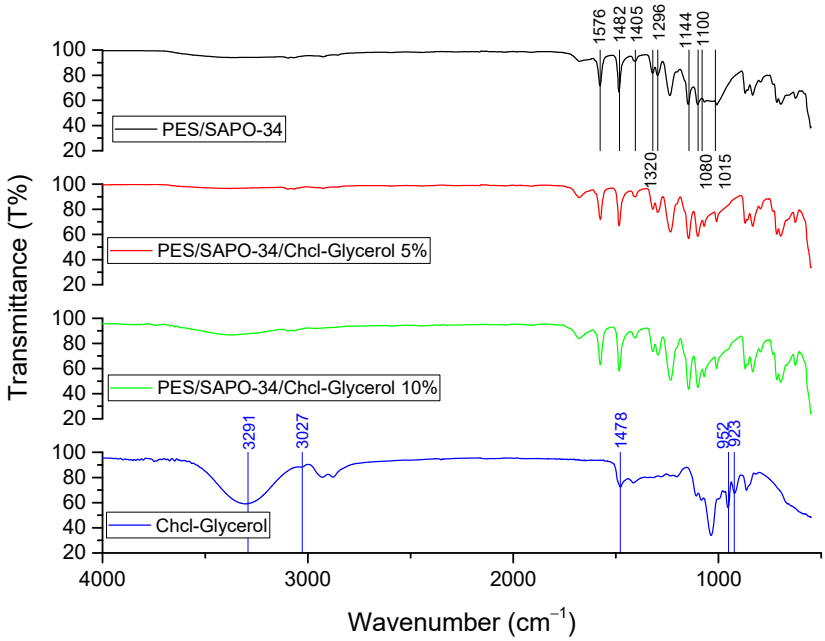

Figure A4. FTIR for PES/SAPO-34 and PES/SAPO-34/ChCl-glycerol membranes.

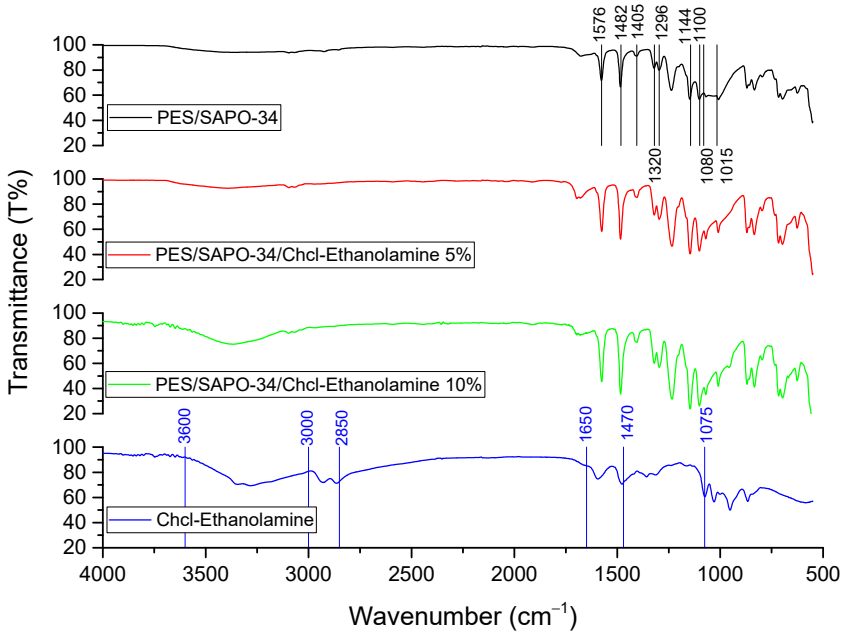

Figure A5. FTIR for PES/SAPO-34 and PES/SAPO-34/ChCl-ethalonamine membranes.

References

1. Comesaña-Gándara, B.; Chen, J.; Bezzu, C.G.; Carta, M.; Rose, I.; Ferrari, M.C.; Esposito, E.; Fuoco, A.; Jansen, J.C.; McKeown, N.B. Redefining the Robeson Upper Bounds for CO_2/CH_4 and CO_2/N_2 Separations Using a Series of Ultrapermeable Benzotriptycene-Based Polymers of Intrinsic Microporosity. *Energy Environ. Sci.* **2019**, *12*, 2733–2740. [CrossRef]
2. Robeson, L.M. Correlation of Separation Factor versus Permeability for Polymeric Membranes. *J. Membr. Sci.* **1991**, *62*, 165–185. [CrossRef]
3. Robeson, L.M. The Upper Bound Revisited. *J. Membr. Sci.* **2008**, *320*, 390–400. [CrossRef]
4. Zimmerman, C.M.; Singh, A.; Koros, W.J. Tailoring Mixed Matrix Composite Membranes for Gas Separations. *J. Membr. Sci.* **1997**, *137*, 145–154. [CrossRef]
5. Bastani, D.; Esmaeili, N.; Asadollahi, M. Polymeric Mixed Matrix Membranes Containing Zeolites as a Filler for Gas Separation Applications: A Review. *J. Ind. Eng. Chem.* **2013**, *19*, 375–393. [CrossRef]

6. Vu, D.Q.; Koros, W.J.; Miller, S.J. Mixed Matrix Membranes Using Carbon Molecular Sieves. *J. Membr. Sci.* **2003**, *211*, 311–334. [CrossRef]
7. Liu, Y.; Takata, K.; Mukai, Y.; Kita, H.; Tanaka, K. Nano-Porous Zeolite and MOF Filled Mixed Matrix Membranes for Gas Separation. *MATEC Web Conf.* **2021**, *333*, 04008. [CrossRef]
8. Tan, X.; Robijns, S.; Thür, R.; Ke, Q.; De Witte, N.; Lamaire, A.; Li, Y.; Aslam, I.; Van Havere, D.; Donckels, T.; et al. Truly Combining the Advantages of Polymeric and Zeolite Membranes for Gas Separations. *Science* **2022**, *378*, 1189–1194. [CrossRef]
9. Liu, B.; Tang, C.; Li, X.; Wang, B.; Zhou, R. High-Performance SAPO-34 Membranes for CO_2 Separations from Simulated Flue Gas. *Microporous Mesoporous Mater.* **2020**, *292*, 109712. [CrossRef]
10. Lu, S.C.; Khan, A.L.; Vankelecom, I.F.J. Polysulfone-Ionic Liquid Based Membranes for CO_2/N_2 Separation with Tunable Porous Surface Features. *J. Memb. Sci.* **2016**, *518*, 10–20. [CrossRef]
11. Ilyas, A.; Muhammad, N.; Gilani, M.A.; Vankelecom, I.F.J.; Khan, A.L. Effect of Zeolite Surface Modification with Ionic Liquid [APTMS][Ac] on Gas Separation Performance of Mixed Matrix Membranes. *Sep. Purif. Technol.* **2018**, *205*, 176–183. [CrossRef]
12. Cardoso, J.S.; Lin, Z.; Brito, P.; Licínio; Gando-Ferreira, M.; Gando-Ferreira, L.M. Surface Functionalized SAPO-34 for Mixed Matrix Membranes in CO_2/CH_4 and CO_2/N_2 Separations. *Sep. Purif. Rev.* **2023**, *52*, 180–193. [CrossRef]
13. Hu, L.; Cheng, J.; Li, Y.; Liu, J.; Zhang, L.; Zhou, J.; Cen, K. Composites of Ionic Liquid and Amine-Modified SAPO 34 Improve CO_2 separation of CO_2-Selective Polymer Membranes. *Appl. Surf. Sci.* **2017**, *410*, 249–258. [CrossRef]
14. Jadav, D.; Bandyopadhyay, R.; Tsunoji, N.; Sadakane, M.; Bandyopadhyay, M. Post-Synthetic Amine Functionalized SAPO-5 & SAPO-34 Molecular Sieves for Epoxide Ring Opening Reactions. In *Proceedings of the Materials Today: Proceedings*; Elsevier Ltd.: Amsterdam, The Netherlands, 2020; Volume 45, pp. 3726–3732.
15. Junaidi, M.U.M.; Khoo, C.P.; Leo, C.P.; Ahmad, A.L. The Effects of Solvents on the Modification of SAPO-34 Zeolite Using 3-Aminopropyl Trimethoxy Silane for the Preparation of Asymmetric Polysulfone Mixed Matrix Membrane in the Application of CO_2 Separation. *Microporous Mesoporous Mater.* **2014**, *192*, 52–59. [CrossRef]
16. Ismail, A.F.; Kusworo, T.D.; Mustafa, A. Enhanced Gas Permeation Performance of Polyethersulfone Mixed Matrix Hollow Fiber Membranes Using Novel Dynasylan Ameo Silane Agent. *J. Membr. Sci.* **2008**, *319*, 306–312. [CrossRef]
17. Mannan, H.A.; Mukhtar, H.; Shahrun, M.S.; Bustam, M.A.; Man, Z.; Bakar, M.Z.A. Effect of [EMIM][Tf2N] Ionic Liquid on Ionic Liquid-Polymeric Membrane (ILPM) for CO_2/CH_4 Separation. *Procedia Eng.* **2016**, *148*, 25–29. [CrossRef]
18. Mannan, H.A.; Mohshim, D.F.; Mukhtar, H.; Murugesan, T.; Man, Z.; Bustam, M.A. Synthesis, Characterization, and CO_2 Separation Performance of Polyether Sulfone/[EMIM][Tf2N] Ionic Liquid-Polymeric Membranes (ILPMs). *J. Ind. Eng. Chem.* **2017**, *54*, 98–106. [CrossRef]
19. Hudiono, Y.C.; Carlisle, T.K.; Bara, J.E.; Zhang, Y.; Gin, D.L.; Noble, R.D. A Three-Component Mixed-Matrix Membrane with Enhanced CO_2 Separation Properties Based on Zeolites and Ionic Liquid Materials. *J. Membr. Sci.* **2010**, *350*, 117–123. [CrossRef]
20. Hudiono, Y.C.; Carlisle, T.K.; LaFrate, A.L.; Gin, D.L.; Noble, R.D. Novel Mixed Matrix Membranes Based on Polymerizable Room-Temperature Ionic Liquids and SAPO-34 Particles to Improve CO_2 Separation. *J. Membr. Sci.* **2011**, *370*, 141–148. [CrossRef]
21. Hu, L.; Zhou, J.; Li, Y.; Cheng, J.; Cen, K.; Liu, J. CO_2 Absorption and Diffusion in Ionic Liquid [P66614][Triz] Modified Molecular Sieves SBA-15 with Various Pore Lengths. *Fuel Process. Technol.* **2018**, *172*, 216–224. [CrossRef]
22. Asghari, M.; Dashti, A.; Rezakazemi, M.; Raji, M.; Sodeifian, G. Polyurethane-SAPO-34 Mixed Matrix Membrane for CO_2/CH_4 and CO_2/N_2 Separation. *Chin. J. Chem. Eng.* **2018**, *27*, 322–334. [CrossRef]
23. Huang, Y.; Yu, M.; Carreon, M.A.; Song, Z.; Zhou, R.; Li, S.; Feng, X.; Zhou, S.J.; Zong, Z.; Meyer, H.S. SAPO-34 Membranes for N_2/CH_4 Separation: Preparation, Characterization, Separation Performance and Economic Evaluation. *J. Membr. Sci.* **2015**, *487*, 141–151. [CrossRef]
24. Rabiee, H.; Meshkat Alsadat, S.; Soltanieh, M.; Mousavi, S.A.; Ghadimi, A. Gas Permeation and Sorption Properties of Poly(Amide-12-b-Ethyleneoxide)(Pebax1074)/SAPO-34 Mixed Matrix Membrane for CO_2, CH_4 and CO_2 Separation. *J. Ind. Eng. Chem.* **2015**, *27*, 223–239. [CrossRef]
25. Jiang, B.; Zhang, N.; Zhang, L.; Sun, Y.; Huang, Z.; Wang, B.; Dou, H.; Guan, H. Enhanced Separation Performance of PES Ultrafiltration Membranes by Imidazole-Based Deep Eutectic Solvents as Novel Functional Additives. *J. Membr. Sci.* **2018**, *564*, 247–258. [CrossRef]
26. Jiang, B.; Zhang, N.; Wang, B.; Yang, N.; Huang, Z.; Yang, H.; Shu, Z. Deep Eutectic Solvent as Novel Additive for PES Membrane with Improved Performance. *Sep. Purif. Technol.* **2018**, *194*, 239–248. [CrossRef]
27. Ma, C.; Sarmad, S.; Mikkola, J.P.; Ji, X. Development of Low-Cost Deep Eutectic Solvents for CO_2 Capture. *Energy Procedia* **2017**, *142*, 3320–3325. [CrossRef]
28. Craveiro, R.; Neves, L.A.; Duarte, A.R.C.; Paiva, A. Supported Liquid Membranes Based on Deep Eutectic Solvents for Gas Separation Processes. *Sep. Purif. Technol.* **2021**, *254*, 117593. [CrossRef]
29. Zhang, Y.; Ji, X.; Lu, X. Choline-Based Deep Eutectic Solvents for CO_2 Separation: Review and Thermodynamic Analysis. *Renew. Sustain. Energy Rev.* **2018**, *97*, 436–455. [CrossRef]
30. John, S.; Wikes; Peter, W.; Tom, W. *Ionic Liquids in Synthesis*; WILEY-VCH Verlags GmbH & Co.: Weinheim, Germany, 2008; Volume 2, ISBN 978-3-527-31239-9.
31. Forsyth, S.A.; Pringle, J.M.; MacFarlane, D.R. Ionic Liquids—An Overview. *Aust. J. Chem.* **2004**, *57*, 113–119. [CrossRef]
32. Castro-Muñoz, R.; Galiano, F.; Figoli, A.; Boczkaj, G. Deep Eutectic Solvents—A New Platform in Membrane Fabrication and Membrane-Assisted Technologies. *J. Environ. Chem. Eng.* **2022**, *10*, 106414. [CrossRef]

33. García, G.; Aparicio, S.; Ullah, R.; Atilhan, M. Deep Eutectic Solvents: Physicochemical Properties and Gas Separation Applications. *Energy Fuels* **2015**, *29*, 2616–2644. [CrossRef]
34. Mero, A.; Koutsoumpos, S.; Giannios, P.; Stavrakas, I.; Moutzouris, K.; Mezzetta, A.; Guazzelli, L. Comparison of Physicochemical and Thermal Properties of Choline Chloride and Betaine-Based Deep Eutectic Solvents: The Influence of Hydrogen Bond Acceptor and Hydrogen Bond Donor Nature and Their Molar Ratios. *J. Mol. Liq.* **2023**, *377*, 121563. [CrossRef]
35. Martins, M.A.R.; Pinho, S.P.; Coutinho, J.A.P. Insights into the Nature of Eutectic and Deep Eutectic Mixtures. *J. Solut. Chem.* **2019**, *48*, 962–982. [CrossRef]
36. Noel Jacob, K.; Senthil Kumar, S.; Thanigaivelan, A.; Tarun, M.; Mohan, D. Sulfonated Polyethersulfone-Based Membranes for Metal Ion Removal via a Hybrid Process. *J. Mater. Sci.* **2014**, *49*, 114–122. [CrossRef]
37. Alenazi, N.; Hussein, M.; Alamry, K.; Asiri, A. Nanocomposite-Based Aminated Polyethersulfone and Carboxylate Activated Carbon for Environmental Application. A Real Sample Analysis. *C* **2018**, *4*, 30. [CrossRef]
38. Du, C.; Zhao, B.; Chen, X.B.; Birbilis, N.; Yang, H. Effect of Water Presence on Choline Chloride-2urea Ionic Liquid and Coating Platings from the Hydrated Ionic Liquid. *Sci. Rep.* **2016**, *6*, 29225. [CrossRef]
39. Rahmalia, W.; Shofiyani, A.; Dewi, Y.S.K.; Septiani, S. Simple Green Routes for Metal-Bixin Complexes Synthesis Using Glycerol-Based Deep Eutectic Solvent. *Indones. J. Chem.* **2022**, *22*, 1759–1767. [CrossRef]
40. Mjalli, F.S.; Murshid, G.; Al-Zakwani, S.; Hayyan, A. Monoethanolamine-Based Deep Eutectic Solvents, Their Synthesis and Characterization. *Fluid Phase Equilibria* **2017**, *448*, 30–40. [CrossRef]
41. Şen, D.; Kalipçilar, H.; Yilmaz, L. Development of Polycarbonate Based Zeolite 4A Filled Mixed Matrix Gas Separation Membranes. *J. Membr Sci.* **2007**, *303*, 194–203. [CrossRef]
42. Cakal, U.; Yilmaz, L.; Kalipcilar, H. Effect of Feed Gas Composition on the Separation of CO_2/CH_4 Mixtures by PES-SAPO 34-HMA Mixed Matrix Membranes. *J. Membr. Scir* **2012**, *417–418*, 45–51. [CrossRef]
43. Wu, T.; Liu, Y.; Kumakiri, I.; Tanaka, K.; Chen, X.; Kita, H. Preparation and Permeation Properties of PeSU-Based Mixed Matrix Membranes with Nano-Sized CHA Zeolites. *J. Chem. Eng. Jpn.* **2019**, *52*, 514–520. [CrossRef]
44. Oral, E.E.; Yilmaz, L.; Kalipcilar, H. Effect of Gas Permeation Temperature and Annealing Procedure on the Performance of Binary and Ternary Mixed Matrix Membranes of Polyethersulfone, SAPO-34, and 2-Hydroxy 5-Methyl Aniline. *J. Appl. Polym. Sci.* **2014**, *131*, 8498–8505. [CrossRef]
45. Zhao, X.; Liu, W.; Liu, X.; Zhang, B. Mixed Matrix Membranes Incorporated with Aminosilane-Functionalized SAPO-34 for Upgrading CO_2/CH_4 Separation Performances. *Ind. Eng. Chem. Res.* **2021**, *60*, 13927–13937. [CrossRef]
46. Cardoso, J.S.; Lin, Z.; Brito, P.; Gando-Ferreira, L.M. The Functionalization of PES/SAPO-34 Mixed Matrix Membrane with [Emim][Tf2N] Ionic Liquid to Improve CO_2/N_2 Separation Properties. *Inorganics* **2023**, *11*, 447. [CrossRef]
47. Sarmad, S.; Xie, Y.; Mikkola, J.P.; Ji, X. Screening of Deep Eutectic Solvents (DESs) as Green CO_2 Sorbents: From Solubility to Viscosity. *New J. Chem.* **2016**, *41*, 290–301. [CrossRef]
48. Cardoso, J.S.; Fonseca, J.P.; Lin, Z.; Brito, P.; Gando-Ferreira, L.M. Optimization and Performance Studies of PES/SAPO-34 Membranes for CO_2/N_2 Gas Separation. *Microporous Mesoporous Mater.* **2023**, *364*, 112845. [CrossRef]